Received: November 26, 2022. Revised: January 7, 2023.

International Journal of
Intelligent Engineering & Systems

http://www.inass.org/

Intensified Convolutional Neural Network for Enhancing Quality of Encrypted and Compressed Optical Images

Jayaseelan Loganathan[1]* **Sureshkumar Chinnaiyan[2]**

[1]*Department of Computer Science, Periyar University, Salem, Tamilnadu, India*
[2]*Paavai College of Engineering, Namakkal, Tamilnadu, India*
* Corresponding author's Email: jayaseelanlphd@gmail.com

Abstract: The compression and encryption of images is essential to securely transmit high quality images over the optical network. In earlier studies, an optical image encryption using Loxodromic cat map with improved double random phase encoding (LCMIDRPE) has been developed. Hilbert huang transform (HHT) used in this encoding model decrease deviations of encrypted images. However, efficient image compression technique is required for compression. An efficient optical image compression and encryption (OICE) technique is developed in this paper by Direction-adaptive discrete wavelet transform (DA-DWT) along with directional lifting and LCMIDRPE. The original image is compressed using the DA-DWT with directional lifting and then encrypted by LCMIDRPE. The inverse version of LCMIDRPE and DA-DWT regain the original image. The missed information's due to lossy compression, decompression, encryption, decryption and transmission of images degrade the quality of regained images. The regained image is enhanced using intensified convolutional neural network (ICNNet). The whole process is termed to be LCMIDRPE-DADWT-ICNNet. Finally, the experimental results exhibits that the LCMIDRPE-DADWT-ICNNet model achieves correlation coefficient (CC) of 0.98 , Peak signal-to-noise ratio (PSNR) of 97db, Mean absolute difference (MAD) of 20 and mean square error (MSE) of 0.45 which is higher than OICE methods like Compressive Sensing and Rivest-Shamir-Adleman method (CS-RSA), Fresnel Diffraction and Discrete Wavelet Transform (FD-DWT), 2Dimentional Sparse Representation and Chaotic Map (2DSR-CM), 2Dimensional Compressive Sensing and Hyperchaotic System (2DCS-HS), Diffractive-Imaging-Based Encryption (DIBE) and Content-Adaptive Image Compression and Encryption using Optimized Compressive Sensing with Double Random Phase Encoding (CAIE-OCS-DPRE) methods.

Keywords: Information exchange, Discrete wavelet transform, Loxodromic cat map, Double random phase encoding, Deep learning method.

1. Introduction

Along with network technological advancements, images now convey a great deal of information. Although bandwidth is constrained and communication methods are inherently unreliable, it is desirable to transfer data that has been compressed and encrypted [1]. The cornerstone of the reduction process is the elimination of spatial and psycho visual redundancy, which can be accomplished with any image compression technique. The compression process can be done either by lossless o by lossy compression. A lossless compression is one in which the image that is recreated from the compressed image is equivalent to the source image [2]

Since, the compression will be insufficient, as it is public accessible and available to everyone. Thus, it should also be secured if it is required, that it can be accessed only by approved individuals. Using symmetric key cryptography (SKC) or asymmetric key cryptography (ASKC), the encryption can be carried out. In SKC, the identical key is utilized for encryption and decryption [3], and distinct keys like public and private keys are employed for encryption and decryption then it is ASKC [4]. Recently, a new concept or technology called compressive sensing (CS) [5] has been established. Comparatively to the conventional method, CS may simultaneously perform sampling and compression. CS and the image encryption technique must be combined in order to accomplish compression and encryption concurrently by utilizing the benefit of CS.

An illustration of CS coding technique for image blocks using CS, which can substantially simplify the compression and reformation of massive data content images. Applying CS theory to detailed image compression, a depth image compression system with superior compression efficiency to JPEG and JPEG2000 is presented [6]. On the basis of CS, a high compression ratio, quick processing approach, and superior reconstructive performance were described for two-dimensional geometric signal compression [7]. The majority of CS-based image compression techniques use the complete measurement matrix as a key, which increases key usage and storage requirements. Additionally, this type of CS-based encryption technique is vulnerable to chosen-plaintext attacks.

In the field of optical image encryption, the double random phase encoding [DRPE] [8], chaos-based image enciphering algorithms [9], have earned a lot of attention. The majority of these encryption techniques sample the original image using CS, which is followed by the chaotic map scattering and diffusing the observed values once more to create the finalized encrypted image. The chaotic system's parameters and beginning values are regarded as its keys. Although these encryption techniques are resistant to chosen-plaintext attacks, higher error between input and output images.

In order to address the aforementioned problems, an OICE-DADWT-LCMIDRPE is developed to enhance the security system with low noise data communication. In this algorithm, the original image is compressed using the DA-DWT with directional lifting for transmission to select the relevant information in image spectrum. Then, the compressed image is enciphered using LCMIDRPE to lower the noise signal ratio and protect the important data.

The Loxodromic Cat Map with double random phase encoding (LCMDRPE) was constructed using this method [10]. When compared to the standard one-degree-of-freedom and quantized cat maps, loxodromic system behaviour is a novel alternative. It has been discovered that the topological integrity has no impact on the quantum periodicity operation. But, the functionality and intricacy of the DPRE were poor and instable. Improved LCMDRPE [11] is presented using a Hilbert huang transform (HHT) rather than a Fourier transform to address this issue. By using this method, the DRPE is improved. This approach is incorporated into the method that is being offered for an effective enciphering system to lower the noise signal ratio and safeguard the pertinent information.

In addition, the real image is retrieved using the inverse versions of LCMIDRPE (decryption) and DA-DWT (decompression). Since, the developed method is a lossy compression, and due to encryption, decryption and transmission of images, some information will be missed out in the reconstructed image. So, the reconstructed image is enhanced using deep learning method like proposed ICNNet. This model composed of different layers. It effectively fixes the issue of gradient disappearance during long-term training. This ICNNet framework incorporates many residual blocks that were initially meant to remove noise from the image, but it was intended for a particular training procedure to improve the image's resolution. The suggested solution is then contrasted with other established approaches for an effective security mechanism with minimal data loss.

The rest of this article is organized as follows: The earlier research on ICE methods is covered in section 2. The proposed methodology is described in section 3, and its effectiveness is shown in section 4. Section 5 summarizes this work and presents suggestions for further improvements.

2. Literature survey

To increase the security of the image encryption system, an OICE-CS-RSA method was devised [12]. However, this method is highly sensitive to noise signals. An ICE algorithm was developed [13] by merging the advanced encryption standard (AES) with the hyper-chaotic system in which Arnold map was used to partially minimize the block effect in an image compression process. So, the encryption time of this approach is increased.

Based on discrete wavelet transform and Fresnel diffraction, the optical ICE technique was presented [14]. More low-frequency data was gathered using Fresnel diffraction. But, this technique have low correlation while measuring linear relationships in pixel-by-pixel intensity between input and output images. Using the CS and Fourier transform, the novel ICE scheme was presented [15] to enhance the security system. However, the compression size of this scheme is high, results in high bandwidth consumption. A protective and effective ICE method was developed [16] by employing CS and a new chaotic structure. However, this method has lower compression ratio.

A multilevel image enciphering/deciphering algorithm was devised [17] using quantum chaos map with sparse sampling. However, the encryption time of this algorithm is high. An ICE approach was presented [18] using 2D sparse representation and chaotic system (ICE-2DSR-CS). On the other hand, narrow and discontinuous range of values used in chaotic system causes differences in input and output images which leads low PSNR.

Double image encryption scheme was developed [19] using CS and DRPE to prevent attackers from decryption. However, this method have low compression ratio in results which cause high bandwidth consumption while transmitting images. ICE based on 2D compressive sensing and hyperchaotic system (ICE-2DCS-HS) was developed [20] for solving the security and efficiency problems image transmission process. Due to high sparsity level used in encryption is sensitive to noise.

Compressed optical image encryption was developed using Diffractive-Imaging-Based Encryption (COIE-DIBE) [21] by input plane and output plane random sampling to improve the security process. However, incorrectly fixed deviation values result in reconstruction error. Content-adaptive image compression and encryption method [22] was presented by optimized compressive sensing with DPRE (CAIE-OCS-DPRE) driven by chaos. However, pixel degradation of this methods lead considerable MSE values.

2.1 Research contribution

The works summarized in literatures have problems like higher bandwidth usage, inadequate security and sensitive towards noise. The main objective of this research work is to provide an efficient scheme for transmitting images with high security and quality. In order to get quality equals to original image, the reconstructed image is further enhanced by deep learning method.

3. Proposed methodology

In this section, effective optimal image compression technique called LCMIDRPE-DADWT is establish for better compression ratio, while maintaining the quality of images. Based on directional lifting, this method locally adjusts the filtering parameters to the image content. The adaptive transform improved energy compression for distinct image characteristics. The developed LCMIDRPE-DADWT approach reduces the frequency that needed to broadcast the compression strategy as a result. While reducing the transmission bandwidth, this method enhances the reliability of optical images. The Fig. 1 represents the schematic representation of the proposed work. The Table 1 depicts the notations used in this research.

Table 1 Notations

X	Input Image sample
Z	Represent integer
m, n	Index to represent image pixel
p, q	Index to represent 4 level decomposition of X
T	Transformation of any matrix
L	Low frequency sub band of wavelet
H	High frequency sub band of wavelet
Π	2-D wavelet orthogonal sampling grid
$\Pi_{p,q}$ (4 sub-grids)	Π_0 - L , Π_1 - H $\Pi_{0,0}$ - LL, $\Pi_{0,1}$ - LH $\Pi_{1,0}$ - HL, $\Pi_{1,1}$ - HH
l_0 ,l_1	even and the odd rows of the image
X_0 X_1	$X[l_0]$ $X[l_1]$
$P_{X,l_1}(.)$	Prediction Function predicts $X[l_1]$ from X_0
$U_{X,l_0}(.)$	Prediction Function that predicts $X[l_0]$ from H
G	Scaling Factor
$u,\ v$	Represent direction of wavelet
c	predicted pixel vale at direction $u,\ v$
d	Directional lifting in $u,\ v$ direction
B	non-overlapping blocks of X
b	Index of block B of X
t, ω	Time frequency dispersion departed from the i^{th} IMF signal
$a_i(t)$	Amplitude values of image pixel
$\omega_i(t)$	Instantaneous frequency
$R_{b,i}$	Number of bits spent on the overhead for selecting $d_{X,b}$
X_2 , X_3, X_4 and X_5	Represent Compressed , encrypted ,decrypted ,decompressed and reconstructed images
h	Hidden matrix in ICNN
x^0	zero-filled image of any image X
λ	Lagrangian multiplier, its value greater than zero
$\mathcal{L}$	Loss function
g_ϑ	ICNNet by loss function for minimum error ϑ
k_s	k – Sequences with s order
r, s	Indexes to represent image index
μ^s	Weight value of hidden layer
w	Represent image samples
γ	step-size

Received: November 26, 2022. Revised: January 7, 2023.

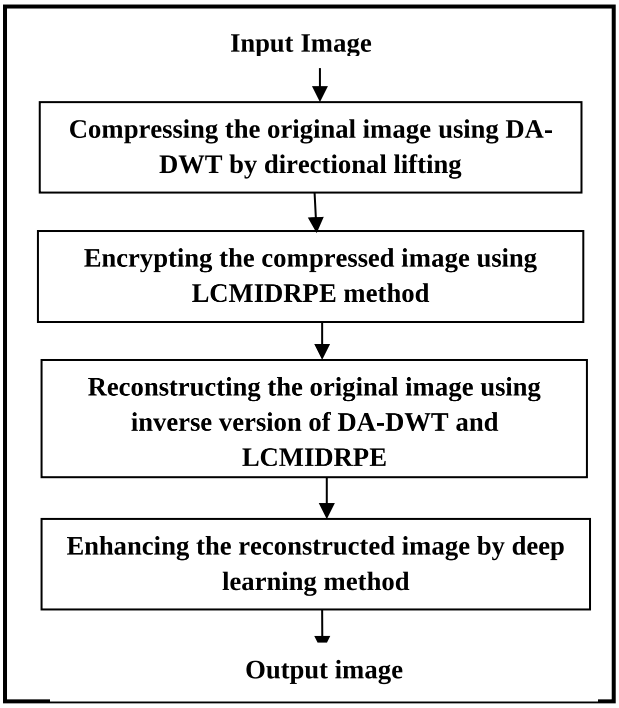

Figure. 1 Schematic representation of the proposed work

3.1 Image compression using DA-DWT

Joint photographic experts groups (JPEG), lossy compression which has the benefits of rapid compression speed and minimal error resultation is mostly used to compress and decompress optical images. This popular compression technique is utilized to select the pertinent data from the visual spectrum. The following are the key steps: The original image is first separated into 8×8 small units of 64 pixels each. The next step is to convert each 8×8 small block using DA-DWT. In the third stage, the quantization table is utilized, with the objective of protecting the low-frequency element and suppressing the high-frequency element. After the DA-DWT transform, the essential information of the image is contained in the upper left corner and disseminated in the lowest right corner. The resultant compressed image data is produced in the fourth stage, which further compresses the information using entropy coding.

3.1.1. 2-D DWT with lifting

Assume, $X = \{X[l] | \, l \in \prod\}$ represent an image of 2-D orthogonal sampling matrix, $X[l] = X[m, n]$ and $l = (m, n)^T$, $\prod = \{(\mathrm{m}, \mathrm{n}) \in \mathbb{Z}^2 | 0 \leq m \leq M - 1, 0 \leq n \leq N - 1\}$
The matrix Π consists of 4 sub-divisions such as Π_{pq} $\{(m, n) \in \prod | \, m \bmod 2 = p, n \bmod 2 = q\}, p, q \; c \; \{0,1\}$.

A transform is performed among the even and odd rows of the image, or between $X_0 = \{X[l_0], l_0 \in \prod_0 = \prod_{00} \cup \prod_{01}\}$ and $X_1 = \{X[l_1], l_1 \in \prod_1 = \prod_{10} \cup \prod_{11}\}$ in order to apply the 2-D DWT on X with directional lifting d. When the resultant low-pass sub-band on $\prod_0$ by $L = \{L[l_0]\} \, 0$ (in Eq. (1)) and the high-pass sub-band on $\prod_1$ will be $\{H[l_1]\}$ (in Eq. (2)), wavelet analysis on X can be written as

$$L[l_0] = G \, . \left(X[l_0] + G . U_{X, l_0}(H) \right), \forall \, l_0 \qquad (1)$$

$$H[l_1] = {}^{1}/_{G} \, . \left(X[l_1] - P_{X, l_1}(X_0) \right), \forall \, l_1 \qquad (2)$$

Where, $P_{X, l_1}(.)$ and $U_{X, l_0}(.)$ are operations that evaluate the input's test values to the output's vector, and G is a scaling factor. Similar to this, wavelet analysis across the even and odd columns of the sample further separates Low-pass sub-band (L**)** into LL defined on $\prod_{00}$ and LH defined on$\prod_{01}$, High-pass sub-band H into HL defined on $\prod_{10}$ and HH defined on $\prod_{10}$ and HH defined on $\prod_{11}$. The division of X into these four sub-bands will be a single level of the 2D-DWT. Typically, this technique is used periodically to the resultant LL sub-band to execute the various stages of the transform.

3.1.2. Direction candidates for directional lifting

With every instance in the wide pass band l_1 for image compression, it is often preferable to utilise a predictive parameter P_{X, l_1} that forecasts $X[l_1]$ from the data in X_0 such that the amplitude of the residual $H[l_1]$is reduced in the detective phase specified in Eq. (1). The preceding equation can be employed in the DA-DWT to choose the $\mathrm{N_c}$ possibilities from which P_{X, l_1} can be determined iteratively Eq. (3),

$$P^{i}_{X, l_1}(X_0) = \sum_{K=0}^{K^P - 1} c_k^p \, . (X[l_1 - (2K + 1)v_i] + X[l_1 - (2K + 1)v_i] \qquad (3)$$

Where $i = 0, \dots . N_c - 1$ and $v_i = \left(v_{i,m}, v_{i,n} \right)$ is defined such that $l_1 \pm (2k + 1)v_i \in \prod_0, \forall \, l_1, \; k = 0, \dots . , K^p - 1$. To take into consideration the areas that are not specified in $\prod$, the symmetrical elongation is specified at image borders like $X \, [-1, 0] = X[1, 0]$. Each candidate should be able to execute wavelet analyses along the stated v_i plane. Indicating the choice of orientation at every data point l_1 as$\widehat{v_{l1}}$. Following the completion of the data identification stage, the relevant upgrade mechanism in Eq. (4).

 DOI: 10.22266/ijies2023.0430.17

$$U_{X,\,l_0}\ (H) \sum_{k=0}^{K^u-1} c_k^u \cdot (\sum_{\{l_1|l_1-(2k+1)\overline{v_{l_1}}=l_0\}} H[l_1] + \sum_{\{l_1|l_1-(2k+1)\overline{v_{l_1}}=l_0\}} H[l_1] \quad (4)$$

Similarly, an image data $X[l_1]$ is predicted by $c_k^p\ X[l_0]$, $L[l_0]$ is updated $c_k^u\ X[l_1]$. For wavelet operations on L and H, additional set of position $u_i = u_{i,m}, u_{i,n}$ is defined such that $l_{01} \pm (2k+1)u_i \in \prod_{00}$ and $l_{11} \pm (2k+1)u_i \in \prod_{10} \forall\ l_{01}, l_{11}, k = 0, \ldots, K^p - 1$.

According to Eqs. (3) and (4), the possibilities for the forecasting component and associated upgrade procedures are constructed in Eq. (4). Due to the assumption that $\acute{v} = (v_y, 2v_x)^T$, directional lifting on on l_0 and l_1 along $\grave{d}_i$ share the identical execution as directional lifting on, provided that and are initially sub-sampled in diagonal by a factor of 2 in vertical position, and then it is transposed.

3.1.3. Adaptive selection of direction and block-partition

The filtering orientations in the DA-DWT must be chosen for image compression to reduce the deformation of the reformed image for a specified rate limit. The delay needed to indicate the selection and the rate for encoding the wavelet parameters are charged for out of the rate budget. Therefore, choosing the ideal direction is comparable to rate-constrained mobility estimated in video processing.

The initial matrix $\prod$ is divided into N_b non-overlapping block, typically every designated by B_b, $b = 0, .., N_b - 1$, for the transform performed to X. Eq. (5) shows the direction $d_{X,b}$ that can be obtained for all B_b by decreasing a lagrangian cost function

$$d_{X,b} = \arg min_i \sum_{l_1 \in \prod l_1 \cap \mathrm{B_b}} [X[l_1] - {P_{X,l_1}^i(X_0)|}/{G} + \lambda\, R_{b,i} \quad (5)$$

The predictive or improved function for each data is described by Eq. (3), Eq. (4), and if $R_{b,i}$ denotes the amount of bits used for overhead while selecting $d_{X,b}$ d it implies that $\widehat{v_{l1}} = v d_{X,b}, \forall\ l_1 \in B_b$. Equivalent definitions are used for the cost functions for the transform on L and H. Though the orientation is chosen block-by-block, the identification and upgrade step's filtering is done over block borders. At balanced data at l at l_0 at block borders may be utilised to recognise the odd instances in several ways. This occurs, for instance, when $|\{l_1 | l_1 + \widehat{v_{l1}} = l_0\}| > 1$. In video coding with motion-compensated periodic filtering, it is comparable to the condition of multiply-connected pixels.

Every block B k may be divided into $2 \times 1, 1 \times 2, 2 \times 2, 4 \times 1, 1 \times 4, 4 \times 2, 2 \times 4\ or\ 4 \times 4$ sub-blocks to enhance the efficiency of the predictive phase. The overhead to indicate the block-partition is incorporated into the cost function in Eq. (5). Then, in a process akin to the variable block-size motion correction in video coding, the best block-partition for every unit and the optimum route for all sub-block that are chosen.

The blocks (sub-blocks) in the proximate neighbourhood are chosen, and the residual is coded using factor-length coding to forecast the route selection. Due to the cyclic nature of the suggested paths, the residual is calculated using regular $\mathrm{N_c}$ arithmetic. The $1\ x\ 1$ segment is enciphered using run-length coding for block-partition decision, whereas the rest use sequence coding. The compressed image is represented as X_2 The Fig. 2 depicts the original (sample) image to compressed images.

3.2 Image encryption using LCMIDRPE

To avoid the problems in secure communication and the information security, the compressed image is encrypted using LCMIDRPE method. Currently, a novel optical image encryption using LCMDRPE [10] is developed. When compared to standard cat maps with one degree of freedom and quantized, loxodromic behaviour is considered as a novel alternative in this procedure.

The constructive firm has been determined that have no effect on the quantum duration value. However, the intricacy and efficiency of the double random phase encoding were poor. Consequently, LCM with Improved DRPE (LCMIDRPE) is used to provide an optical image encryption [11]. Then, Hilbert Huang Transform (HHT) is introduced to improve the enciphered functions which is mathematically described in Eq. (6)

$$HHT(t,\omega) = \sum_{i=1}^{n} HHT_i(t,\omega) \equiv \sum_{i=1}^{n} a_i(X_2\ (t,\omega_i)) \quad (6)$$

where $HHT_i(t,\omega)$ is the time frequency dispersion departed from the signal's the i^{th} Intrinsic Mode Functions (IMF). The symbol ≡ denotes 'by description,' and $a_i(t,\omega_i)$ integrates the signal's amplitude $a_i(t)$ and instantaneous frequency $\omega_i(t)$ from the input X_2 Fig. 2 demonstrates the transformation of compressed images to enciphered images. Finally, the encrypted image is represented

Received: November 26, 2022. Revised: January 7, 2023.

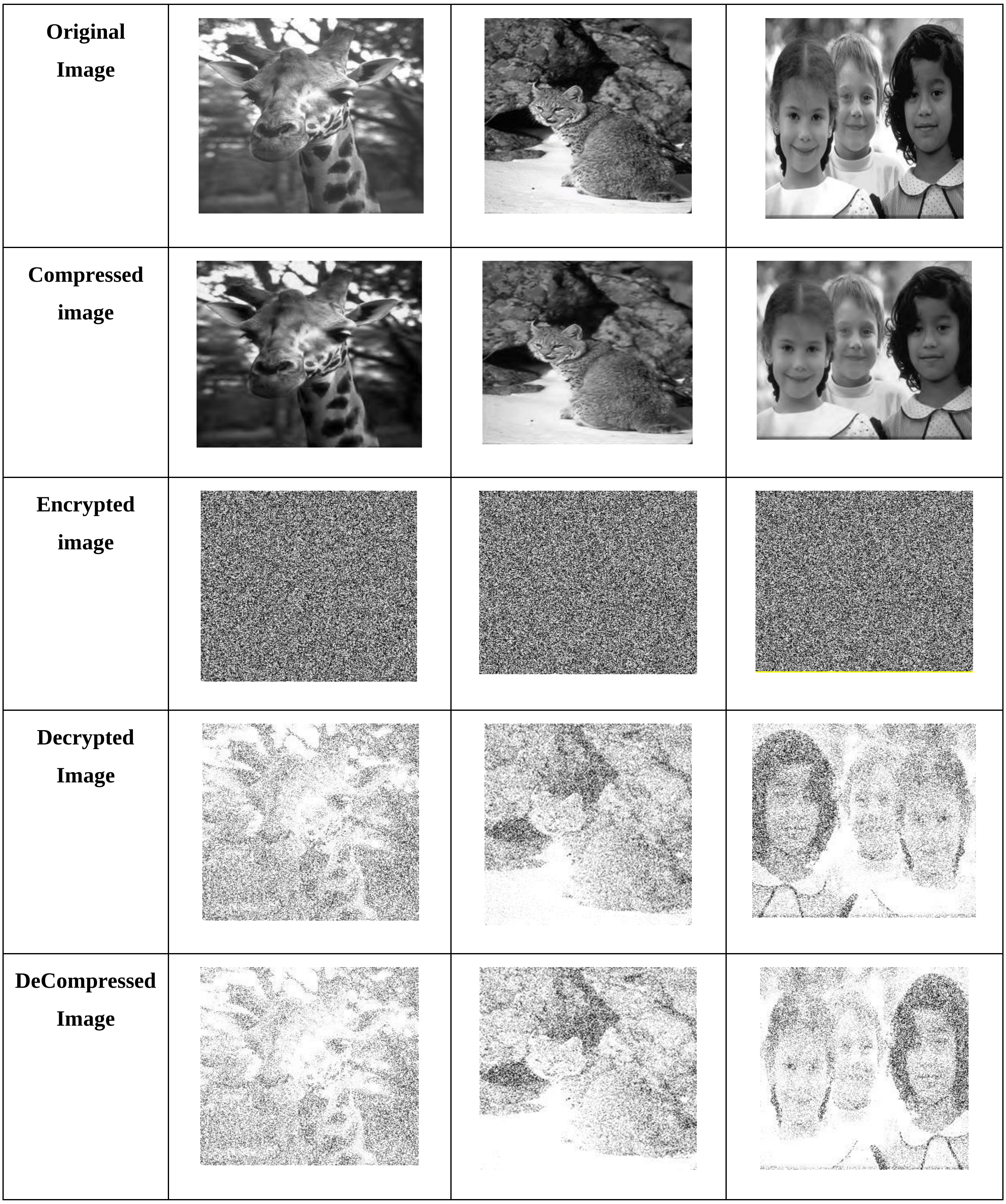

Figure. 2 Compressed images to encrypted images

as X_3. Fig. 2 demonstrates the transformation of compressed images to enciphered images.

3.3 Image decryption using ILCMIDRPE

Once the encrypted process is completed using LCMIDRPE method, the decryption process is computed. The decryption operation is the inverse function is used to retrieve the original image for sparse recovery. For this process, the Inverse Hilbert Huang Transform (IHHT) is used to decrypt the images which is defined as Eq. (7)

$$IHHT(t,\omega) = -\sum_{i=1}^{n} HHT_i(t,\omega) \equiv -\sum_{i=1}^{n} a_i X_3(t,\omega_i)) \quad (7)$$

where $IHHT_i(t,\omega)$ is the inverse time frequency dispersion depicted from the signal's i^{th} IMF. Finally, the decrypted image is represented as X_4 Fig. 2 shows the transformation of an encrypted image into a deciphered image.

3.4 Image de-compression using DA-IDWT reconstruction

The DA-IDWT is taken to decompress the final decrypted image. The decompression process is the vice-versa of the developed compression process. In this process, DA-IDWT is applied on each obtained block and uses the assigned values from the compressed image to form the new image in the same dimensions for the real image. The decompressed image is represented as X_5. The Fig. 2 depicts the deciphered image to decompressed image.

3.5 Enhancing the reconstructed image using ICNNet model

Generally, lossy compression, encryption, transmission of images, decryption and decompression process leads to quality degradation of images. In order to solve this issue, intensified convolutional neural network (ICNNet) is used to recover the distorted image information.

The suggested ICNNet model efficiently handles gradient vanishing concerns during the durable training phase to provide effective image quality pixel improvement. ICNNet for image enhancement is made up of numerous residual layers that were initially intended to remove noise from images, but it is now specifically built for training to increase image resolution or reliability. The total level of the neural network is 20. The first layer is convolution (convo) + rectified linear unit (ReLU), the second through eighteenth layers are convolution + batch normalization (BN) + ReLU and the final layer is convolution with an added layer of back-propagation (BP) and loss.

The most important aspect of the entire ICNNet network design is that after training a series of image samples for obtaining the quality. The decompressed image is given as the test image to improve the quality. As a result, the original high-resolution image may be recreated by improving the quality from trained model of ICNNet.

The ICNNet is type of deep learning method propose in this research work. For the image enhancement process, $\widehat{X4}_{r,s}$ with every sample set insisting of an autonomous sampling structure and dimension criteria's. For this, ICNNet is trained through Eq. (8) as,

$$X_5 = \underset{\vartheta}{arg\,min} \sum_{r.s,s'} \mathcal{L}\left(g_\vartheta\left(\widehat{X4}_{r,s}\right) \widehat{X4}_{r,s}{}'\right) \quad (8)$$

Algorithm 1: ICNN for enhancing the image quality.
Input: initialize $x_4^0 = r^0 \in R^N$ (decompress samples) and $\gamma > 0, \{\mathrm{k_s}\}_{\mathrm{s \in n}}$ **Output:** Enhanced reconstructed image $\mathrm{X_5}$ For $s = 1,2, \ldots do$, $\mu^s \rightarrow r^{s-1} - \gamma\, h(x_4^s)$ $x_5^s = ICNNet\,(\mu^s)$ $k_s \leftarrow \frac{1}{2}\left(1 + \sqrt{1 + Nk_{s-1}^n}\right)$ $\mathrm{r^s} \leftarrow \mathrm{x_5^s} + \left(\frac{\mathrm{k_{s-1}} - 1}{\mathrm{k_s}}\right))\,)(\mathrm{x_5^s} - \mathrm{x_5^{s-1}})$ End

Additionally, back propagation is employed to remove the dependency of DL on fully-sampled dimensions. ICNNet learning was complicated by the necessity of several and validated training image samples from the identical sample, which hindered the process further.

Assume, an image pixel X_4 with parameters of r and s integer width and height is represented by the notation $X_4(r,s)$ in Eq. (9) represents the hypothesis that testing requirements are uncorrelated in any subset of 2 by 2 area.

$$X_5(r,s) = \left\{\widehat{X4}\,(r,s), \widehat{X4}\,(r+1,s), \widehat{X4}\,(r,s+1), \widehat{X4}\,(r+1,s+1)\right\} \quad (9)$$

By mapping every observed variance as $h_{\widehat{X4}}$ of the associated zero-filled image to the other, an ICNN is evaluated with the decompressed images using a sampled measurement parameter b as an isolated testing sample. The decompressed image with same measurement criteria is given as input to the ICNNet process and the training procedure is continued with multiple sampled parameters from various samples (n) and by eliminating the following statistical concern, the Eq. (9) is improved as Eq. (10)

$$X_5(r,s) = \underset{\vartheta}{\arg min} \sum_i \sum_{w,w'}^{h_{\widehat{X4}}^x} \mathcal{L}\left(g_\vartheta\,(w)\, w'\right) \quad (10)$$

In Eq. (10), w is the indexes with various learning subjects, g_ϑ is the ICNNet parameterized by using ϑ. w and w' are two different subjects for training sample set. $h_{\widehat{X4}}^x$ represents the x^{th} zero-filled image of $\mathrm{X_4}$

Therefore, by introducing ICNNet model the decompressed images are reconstructed with enhanced quality. The topology of ICNNet is presented in Fig. 3. The missing information due to cryptography and compressing is restored from the

Received: November 26, 2022. Revised: January 7, 2023.

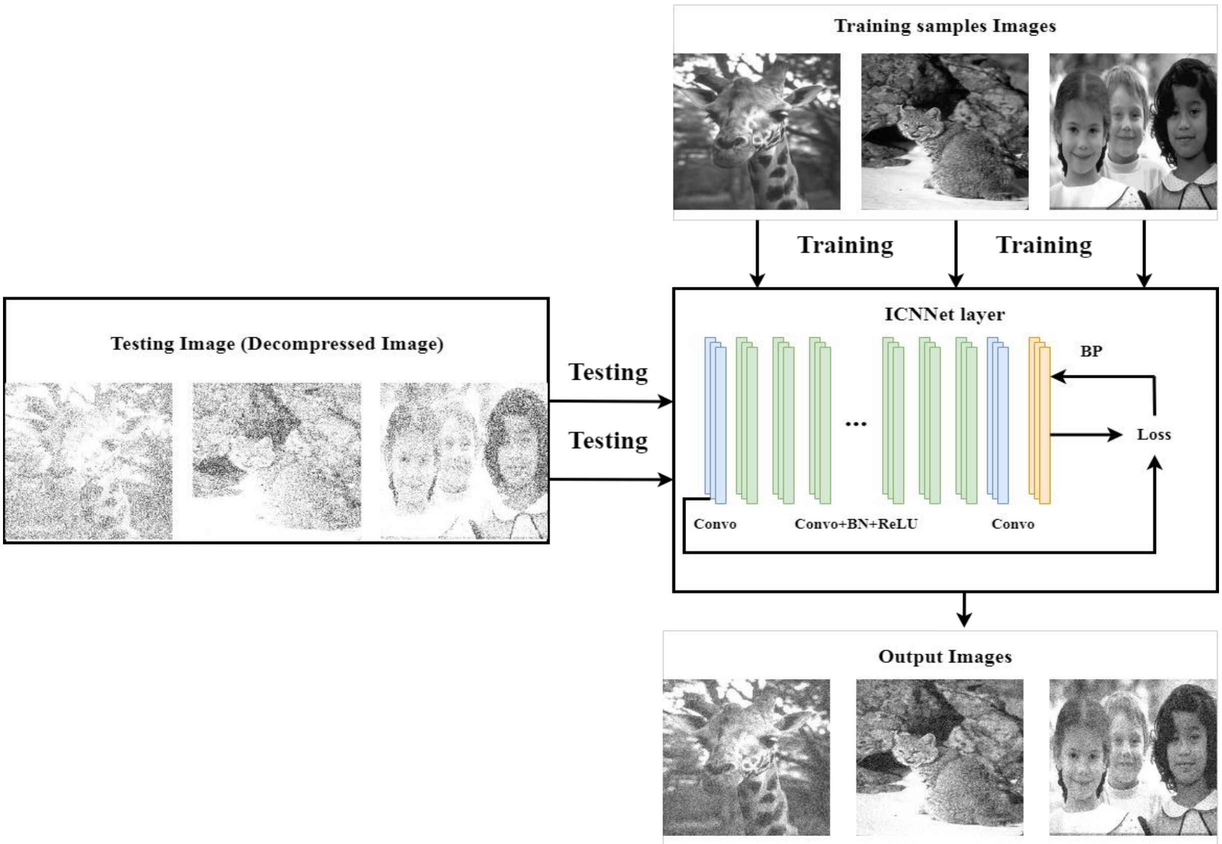

Figure. 3 ICNNet for enhancing the image quality

ICNNet trained model iteratively until obtain maximum quality.

4. Result and discussion

The proposed and existing works for input image are implemented in MATLAB 2017. The existing methods OICE-CS-RSA [12], OICE-FD-DWT [14] ICE-2DSR-CM [18] ICE-2DCS-HS [20], COIE-DIBE [21] and CAIE-OCS-DPRE [22] are compared to the proposed in terms of correlation coefficient, mean absolute difference, peak signal-to-noise ratio and mean square error.

4.1 Correlation coefficient (CC)

It is a measure that gives the correlation between related elements in the original image and the enhanced reconstructed image. It is computed as follows from Eq. (11) to Eq. (16)

$$r_{X,X_5} = \frac{c_v(X, \mathrm{X}_5)}{\sigma_X \, \sigma_{X_5}} \tag{11}$$

$$\sigma_X = \sqrt{\frac{1}{N}\sum_{i=1}^{N}\left(X_i - E(X_i)\right)^2} \tag{12}$$

$$\sigma_{\mathrm{X}_5} = \sqrt{\frac{1}{N}\sum_{i=1}^{N}\left({X_5}_i - E\left(y\, {X_5}_i\right)\right)^2} \tag{13}$$

$$E(X) = \frac{1}{N}\sum_{i=1}^{N}(X_i) \tag{14}$$

$$E(X_5) = \frac{1}{N}\sum_{i=1}^{N}\left({X_5}_i\right) \tag{15}$$

$$c_v(X, X_5) = \frac{1}{N}\sum_{i=1}^{N}\left(X_i - E(X_i)\right)\left({X_5}_i - E\left({X_5}_i\right)\right) \tag{16}$$

Here, N is the total number of images, $c_v(X, \mathrm{X}_5)$ denotes the covariance between the original image X and X_5, σ_X and σ_{X_5} are the variances of X and X_5. Also, $E(X)$ and $E(X_5)$ are the mean values of X and X_5. A better image quality is indicated by the high value of CC.

Fig. 4 compares the LCMIDRPE-DADWT-ICNNet in terms of CC with other existing methods. The LCMIDRPE-DADWT-ICNNet achieves 0.98% CC in this analysis, while the other techniques have lower CC values. Thus, it is proved the suggested method provide quality output.

4.2 Mean absolute difference (MAD)

MAD is defined as the ratio of sum of all absolute values of deviation from original and enhanced reconstructed image to the total number of given image samples. The formula is given in Eq. (17).

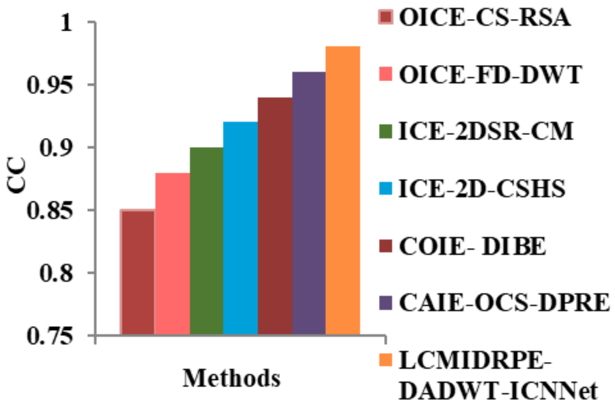

Figure. 4 Evaluation of CC

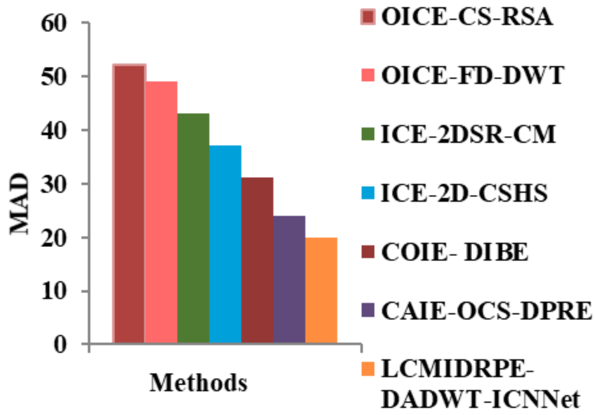

Figure. 5 Evaluation of MAD

$$MAD = \sum_{i=1}^{N} \frac{|X_i - X_{5i}|}{N} \quad (17)$$

Where, X_i is the original image; X_{5i} is the enhanced reconstructed image; N is the number of image sample.

Fig. 5 compares the LCMIDRPE-DADWT-ICNNet technique with different methods in terms of MAD.The proposed LCMIDRPE-DADWT-ICNNet has been resulted with 20 MAD which is lower than other techniques. It demonstrates that the proposed approach offers reconstructed image with less MAD value.

4.3 Mean square error (MSE)

The average of the squared error rates among the values of the actual and reconstructed image known as MSE in Eq. (18),

$$MSE = \frac{1}{MN} \sum_{x=1}^{M} \sum_{y=1}^{N} |X(x,y) - X_5(x,y)|^2 \quad (18)$$

The image dimensions in this case are M and N.

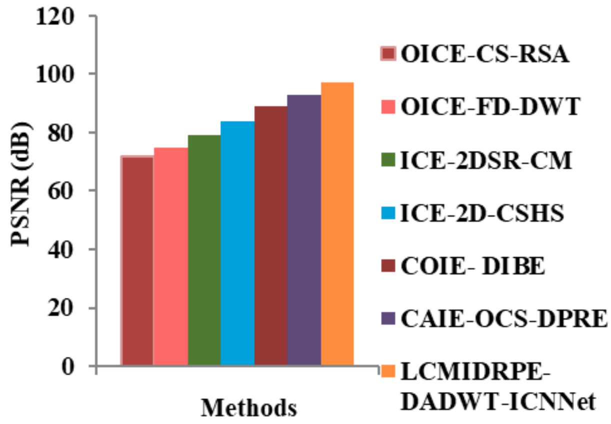

Figure. 6 Evaluation of PSNR

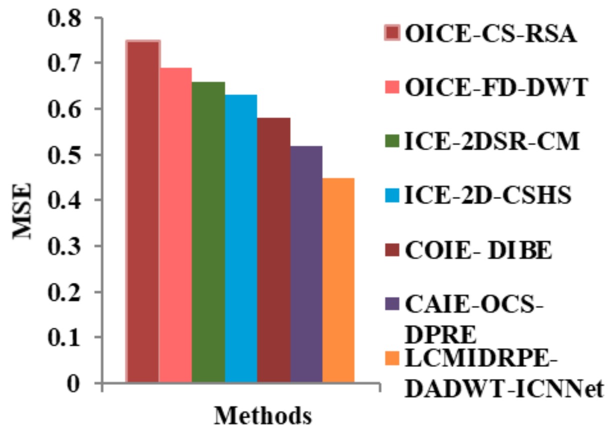

Figure. 7 Evaluation of MSE

Fig. 7 shows that the comparison of LCMIDRPE-DADWT-ICNNet with other approaches in terms of MSE. LCMIDRPE-DADWT-Innes has 0.45 whereas the other approaches have higher MSE values. Thus, results proved that LCMIDRPE-DADWT-ICNNet provides output images with lower MSE values.

4.4 Peak signal-to-noise ratio (PSNR)

By utilizing the MSE value, the PSNR is calculated as follows Eq. (19).

$$PSNR = 10log_{10}\left(\frac{255^2}{MSE}\right) \quad (19)$$

Fig. 6 shows that the comparison of LCMIDRPE-DADWT-ICNNet with other methods by PSNR. The X-axis represents the techniques. Y-axis represents the PSNR value. LCMIDRPE-DADWT-ICNNet has 97 dB whereas the other approaches have less PSNR values. Therefore, it proves that the LCMIDRPE-DADWT-ICNNet approach provides better encryption with maximized PSNR values.

Received: November 26, 2022. Revised: January 7, 2023.

Table 2. Comparison of encryption time, compression ratio and bandwidth occupancy

Methods	Encryption time (ms)	Compression ratio	Bandwidth occupancy (%)
ICE-AES	350	1	20
ICE-CS-FT	310	1.5	18.5
ICE-CS-NCS	265	2.3	14.3
IED-QCM-SS	222	3.4	12.9
DIES-CS-DRPE	194	4.2	12.1
LCMIDRPE-DADWT-ICNNet	150	5.0	10.2

4.5 Additional metrics

The encryption time or speed, Compression ratio and Bandwidth occupancy are evaluated in this section. The encryption time or speed is the actual time taken for enciphering image. Compression ratio is the ratio between the sizes of uncompressed image to size of compressed image. Bandwidth occupancy of compressed image is measured in the local area network using NetFlow Analyzer [23].

The below Table 2 depicts comparison of proposed model with image compression and encryprtion using advanced encryption standard (ICE-AES) [13], image compression and encryprtion using compression sensing and fourier transform (ICE-CS-FT) [15], image compression and encryprtion using compression sensing with new chaotic structure (ICE-CS-NCS) [16], image encryption and decryption using quantum chaos map with sparse sampling. IED-QCM-SS [17] and double image encryption scheme using CS and DRPE (DIES-CS-DRPE) [19]

From the above Table 2, it is observed that the proposed LCMIDRPE-DADWT-ICNNet model provides better Encryption, compression ratio and bandwidth occupancy. For instances, the proposed model achieves 57.14%, 51.61%, 43.39%, 32.43% and 22.68% lesser encryption speed (s) than ICE-AES, ICE-CS-FT, ICE-CS-NCS, IED-QCM-SS and DIES-CS-DRPE. Also, the LCMIDRPE-DADWT-ICNNet model achieves higher compression than other models. Similarly, the proposed LCMIDRPE-DADWT-ICNNet model achieves lesser bandwidth occupancy than the other models. This evaluation is proved that the proposed models is suitable for secure sharing of images in optical network with less encryption time, compression size and bandwidth occupancy than other existing models.

5. Conclusion

In this research work, optical ICE methods have been developed using DA-DWT via directional lifting and LCMIDRPE. The original image is compressed using the DA-DWT with directional lifting then the compressed image is enciphered using LCMIDRPE secure images in transmission. The IDA-DWT and ILCMIDRPE is used to retain the original image. The developed method is a lossy compression, and also due to encryption, decryption and transmission process of images, some information may be missed out in the reconstructed image. So, the reconstructed image is enhanced using deep learning method. The test outcomes of LCMIDRPE-DADWT-ICNNet provides 0.98 of CC 97 dB of PSNR, 20 MAD and 0.45 value of MSE which is are better than the other existing models. This provides the efficiency of proposed model help to send images in network by securing and preserving the image quality. In future, an optimized chaotic method will be investigated for further improving security of optical images.

Conflict of interest

The authors declare no conflict of interest.

Author contributions

Conceptualization, methodology, software, validation, Jayaseelan; formal analysis, investigation, Sureshkumar; resources, data curation, writing—original draft preparation, Jayaseelan; writing—review and editing, Jayaseelan; visualization; supervision, Sureshkumar;

Reference

[1] S. M. Hilles and M. A. Salem, “Selective image encryption and compression technique”, *Arrasikhun Journal*, Vol. 4, No. 1, pp. 39-42, 2018.

[2] M. Singh, S. Kumar, S. Singh and M. Shrivastava, “Various image compression techniques: Lossy and lossless”, *International Journal of Computer Applications*, Vol. 142, No. 6, pp. 23-26, 2016.

[3] R. Ge, G. Yang, J. Wu, Y. Chen, G. Coatrieux, and L. Luo, “A novel chaos-based symmetric image encryption using bit-pair level process”, *IEEE Access*, Vol. 7, pp. 99470-99480, 2019.

[4] H. Shuihua and Y. Shuangyuan, “An asymmetric image encryption based on matrix transformation”, *ECTI Transactions on Computer and Information Technology (ECTI-CIT)*, Vol. 1, No. 2, pp. 126-133, 2005.

[5] D. L. Donoho, “Compressed sensing”, *IEEE Transactions on Information Theory*, Vol. 52, No. 4, pp. 1289-1306, 2006.

[6] M. Sarkis and K. Diepold, "Depth map compression via compressed sensing", In: *Proc. of 2009 16th IEEE International Conference on Image Processing (ICIP)*, pp. 737-740, 2009.

[7] D. Z. Ming and G. G. Hua, "2-D geometric signal compression method based on compressed sensing", In: *Proc. of 2011 International Conference on Electronics, Communications and Control (ICECC)*, pp. 601-604, 2011.

[8] B. Deepan, C. Quan, Y. Wang, and C. J. Tay, "Multiple-image encryption by space multiplexing based on compressive sensing and the double-random phase-encoding technique", *Applied Optics*, Vol. 53, No. 20, pp. 4539-4547, 2014.

[9] M. Elshamy, A. N. Rashed, A. E. N. A. Mohamed, O. S. Faragalla, Y. Mu, S. A. Alshebeili, and F. E A. E. Samie, "Optical image encryption based on chaotic baker map and double random phase encoding", *Journal of Lightwave Technology*, Vol. 31, No. 15, pp. 2533-2539, 2013.

[10] L. Jayaseelan and C. Sureshkumar, "An Optical Image Encryption Using Loxodromic Cat Map With Double Random Phase Encoding (LCMDRPE)", *Int J Recent Sci Res*, Vol. 8, No. 8, pp. 18946-18950, 2017.

[11] L. Jayaseelan and C. Sureshkumar, "An Optical Image Encryption Using Loxodromic Cat Map With Improved Double Random Phase Encoding (LCMIDRPE)", *International Journal of Advanced Research in Computer Science*, Vol. 8, No. 8, pp. 107-110, 2017.

[12] L. Gong, K. Qiu, C. Deng, and N. Zhou, "An optical image compression and encryption scheme based on compressive sensing and RSA algorithm", *Optics and Lasers in Engineering*, Vol. 121, No. 169-180, 2019.

[13] Z. Nie, Z. X. Liu, X. T. He, and L. H. Gong, "Image compression and encryption algorithm based on advanced encryption standard and hyper-chaotic system", *Optica Applicata*, Vol. 49, No. 4, 2019.

[14] C. Wu, J. Chang, C. Quan, X. Zhang, and Y. Zhang, "The optical image compression and encryption method based on fresnel diffraction and discrete wavelet transform", *Results in Optics*, Vol. 1, p. 100021, 2020.

[15] M. Zhang, X. J. Tong, J. Liu, Z. Wang, J. Liu, B. Liu, and J. Ma, "Image compression and encryption scheme based on compressive sensing and Fourier transform", *IEEE Access*, Vol. 8, pp. 40838-40849, 2020.

[16] Y. Tang, M. Zhao, and L. Li, "Secure and efficient image compression-encryption scheme using new chaotic structure and compressive sensing", *Security and Communication Networks*, Vol. 2020, No. 2, pp. 1-15, 2020.

[17] R. K. Singh, B. Kumar, D. K. Shaw and D. A. Khan, "Level by level image compression-encryption algorithm based on quantum chaos map", *Journal of King Saud University-Computer and Information Sciences*, Vol. 33, No. 7, pp. 844-851, 2021.

[18] A. Ghaffari, "Image compression-encryption method based on two-dimensional sparse recovery and chaotic system", *Scientific Reports*, Vol. 11, No. 1, pp. 1-19, 2021.

[19] R. Zhang and D. Xiao, "Double Image Encryption Scheme Based on Compressive Sensing and Double Random Phase Encoding", *Mathematics*, Vol. 10, No. 8, p. 10.3390/math10081242, 2022.

[20] J. Liu, M. Zhang, X. Tong, and Z. Wang, "Image compression and encryption algorithm based on 2D compressive sensing and hyperchaotic system", *Multimedia Systems*, Vol. 28, No. 2, pp. 595-610, 2022.

[21] S. Wan, Q. Gong, H. Wang, S. Ma, and Y. Qin, "Compressed optical image encryption in the diffractive-imaging-based scheme by input plane and output plane random sampling", *Optica Applicata*, Vol. 52, No. 1, pp. 51-66, 2022.

[22] Z. Gan, X. Chai, J. Bi and X. Chen, "Content-adaptive image compression and encryption via optimized compressive sensing with double random phase encoding driven by chaos", *Complex & Intelligent Systems*, Vol. 8, No. 3, pp. 2291-2309, 2022.

[23] https://www.manageengine.com/products/netflow/